OnionCode: Enabling Multi-priority Coding in LED-based Optical Camera Communications

Haonan Wu †&, Yi-Chao Chen †&, Guangtao Xue†*, Yuehu Jiang †, Ming Wang‡, Shiyou Qian†, Jiadi Yu†, Pai-Yen Chen♦
† Department of Computer Science and Engineering, Shanghai Jiao Tong University, China
‡ Department of Mathematics, University of Illinois at Urbana-Champaign, USA
♦ Department of Electrical and Computer Engineering, University of Illinois at Chicago, USA
Email:{haonanwu,yichao,xue-gt}@sjtu.edu.cn,mingw4@illinois.edu,{qshiyou,jiadiyu}@sjtu.edu.cn,pychen@uic.edu

***Abstract*—Optical camera communication (OCC) has attracted increasing attention recently thanks to the wide usage of LED and high-resolution cameras. The lens-image sensor structure enables the camera distinguish light from various source, which is ideal for spatial MIMO. Hence, OCC can be applied to several emerging application scenarios, such as vehicle and drone communications. However, distance is a major bottleneck for OCC system, because the increase in distance makes it difficult for the camera to distinguish adjacent LED, which we call LED spatial mixing.**

In this paper, we propose a novel hierarchical coding scheme name as OnionCode to support dynamic range of channel capacity in one-to-many OCC scenario. OnionCode adopts a multi-priority receiving scheme, i.e., the receivers can dynamically discard the low-priority bit stream according to the measured channel capacity. OnionCode achieves this based on a key insight that, the luminance level of a mix-LED is distinguishable. We prototype an LED-based OCC system to evaluate the efficacy of OnionCode and the results show that OnionCode achieves a higher conding efficiency and overall throughput compared with the existing hierarchical coding.

Index Terms*—*optical camera communications; hierarchical coding; one-to-many transmission;

I. Introduction

Scarce and congested spectrum has become a major bottleneck in traditional RF communications. Visible light communication (VLC) has become a promising complement thanks to the widely deployed LED infrastructure and abundant spectrum resources. Compared with the photodiode (PD)-based VLC systems, optical camera communications (OCC) [1] utilize the off-the-shelf image sensors as the receiver, which are commonly used in smartphones, digital cameras, vehicle/drone-mounted cameras, etc. The most attractive feature of the OCC system is the spatial MIMO. Specifically, an image sensor can be viewed as a two-dimensional PD array and the lens can separate different light sources spatially on the two-dimensional plane of the sensor. Thanks to the high resolution image sensor and light-source-separating lens, OCC system can provide high SNR by discarding the pixels associated with ambient noise which can be achieved by computer vision techniques. In summary, the lens-image sensor structure is able to establish parallel and high quality channels between the transmitter and receiver.

& Both authors contributed equally to the research.
* Corresponding author.

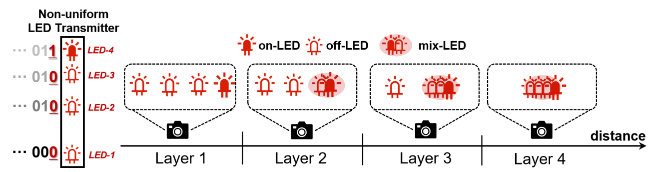

(a) Concept of one-to-many transmission and LED spatial mixing.

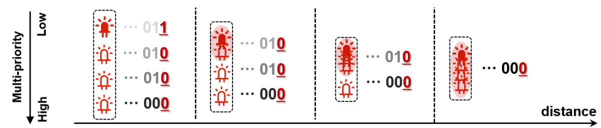

(b) Concept of multi-priority receiving.

Fig. 1. OnionCode: (a) Multiple receivers at various distance can receive the bits transmitted by the transmitter simultaneously and the receiver cannot distinguish the luminance of each LED due to spatial mixing; (b) The receiver selectively discards low-priority bit stream according to the mixing status.

Hence, there is growing interest in OCC applications and many works have been proposed in scenarios such as visible light positioning (VLP) [2]–[4], screen-camera communication [5]–[10], V2V/V2I (V2X) communication [11]–[15], and drone-camera communication [16]–[18], etc. Among these works, OCC particularly shows great advantage in scenarios requiring one-to-many communications. For example, in V2X, a traffic light can broadcast traffic conditions to all vehicles toward it; in visible light positioning, a programmable light can broadcast location or location-based information to users holding their phones.

However, in the above-mentioned OCC applications, the communication distance is a crucial performance metric. As discussed in [19], the optical cameras have limited resolving power described by the Rayleigh criterion. In other words, if the LED-to-camera distance is large enough, the camera cannot spatially separate LED light sources that are close together which is termed as *LED spatial mixing*, as shown in Fig. 2(b).

LED spatial mixing can significantly impair the efficiency of OCC one-to-many communications. As shown in Fig. 1(a), if a camera (i.e., a receiver) is close to the LED transmitter, the LEDs can be clearly distinguished, resulting in higher channel capacity. As the distance increases, the channel capacity will decrease due to stronger spatial mixing. Thus, in a one-to-many communication, if the transmitter sends at the data rate of the nearest receiver, the more distant receiver affected by spatial mixing will not receive any data; on the other hand, if the transmitter limits the data rate according to the farthest receiver, it wastes part of the channel capacity of the closer receivers.

To address the issue, *hierarchical coding* [9], [13] schemes are proposed to support dynamic range of channel capacity. Hierarchical coding is a physical layer coding that allows receivers at various distances to dynamically adjust the receiving rate according to the measured channel capacity. That is, the LED transmitter encodes data at a fixed rate. Receivers at a shorter distance can retrieve more data and achieve a higher throughput; receivers at a larger distance and suffering from spatial mixing, instead of losing all data, can still decode part of the information.

Despite the great potential for application in OCC one-to-many communication, the existing hierarchical coding scheme [13] still suffers from low coding efficiency. In this paper, we propose a novel non-block-based hierarchical coding scheme, called ONIONCODE, which achieves higher coding efficiency. We show that ONIONCODE can fully utilize the channel capacity of receivers at different distances (i.e., with different levels of spatial mixing) without injecting any redundancy to the transmitted data. The key idea to achieve high coding efficiency is based on the observation that we can assume dependencies among the messages of all receivers without degrading the practicality of OCC one-to-many communication. Therefore, ONIONCODE adopts a *multi-priority receiving* shown in Fig. 1(b), i.e., a specific priority is assigned to the bit stream transmitted by each LED, and the remote receiver discards the low-priority stream layer by layer, because of which we named it as ONIONCODE. For example, a short-distance receiver (layer 1) can reserve all 4 streams without data rate loss, but a long-distance receiver (layer 4) cannot decode 3 low-priority streams due to severe mixing.

A *key insight* of ONIONCODE is that the camera cannot distinguish which LED is lit , but it can determine how many LEDs are lit in the case of LED mixing. Hence, we formulate the LED spatial mixing and set up the concept of layer. Then, we modeled the coding space of each layer according to the key insight, and design a unique encoding table for the transmitter and decoding table for the receiver of each layer, in order to achieve multi-priority receiving. The most prominent advantage of ONIONCODE is the higher coding efficiency compared with the existing overlay coding [13], ONIONCODE does not sacrifice the data rate of the nearest receiver and greatly improves the overall throughput in one-to-many communication scenario.

Applying ONIONCODE to the actual OCC system poses a number of challenges. First, accurate frame synchronization and pixel-level channel segmentation are prerequisites for high-quality communication, which should be achieved with the lowest communication and computational overhead (Sec. V-C1 and Sec.V-C2). Second, the camera's exposure parameters are highly related to the quality of the optical channel. In order for cameras of different layers to achieve the optimal SNR, an adaptive parameters adjustment mechanism is needed (Sec. V-C3). Third, the spatial aliasing at the receiver of different layers is various. We need to design a uniform channel estimation scheme for all layers to minimize the overhead of channel estimation (Sec. V-C4).

ONIONCODE can be applied to mobile OCC communication scenarios such as V2X and drone communication. The details of applications is discussed in Sec.VII. The main contribution of ONIONCODE can be summarized as follows:

- We propose ONIONCODE, a novel hierarchical coding scheme that allows the receiver to receive multi-priority bit streams adaptively according to the channel capacity without adding extra bits to the transmitted data, thus achieving higher coding efficiency than existing coding schemes.
- A variety of communication mechanisms are proposed including frame synchronization, fine-grained LED segmentation, adaptive camera configuration and channel estimation, to ensure low overhead and high SNR.
- We implement ONIONCODE using COTS digital camera and LED light source. Evaluation results demonstrate the efficacy of ONIONCODE and show that the throughput of ONIONCODE outperforms that of the state-of-the-art coding scheme by 67%.

II. RELATED WORK

A. Optical Camera Communication(OCC)

LED-based OCC technologies have attracted great interest in recent years. The LED-based OCC has been applied to several emerging application scenarios. VLC on drones was first discussed in [18] and [16], [17] implemented drone-ground communication prototype utilizing drone-mounted LED array and ground camera. The LEDs of **V**ehicles and traffic related **I**nfrastructure were used as the transmitter in V2V/V2I communications [12], [20]. Visible light positioning (VLP) is another novel application of LED-based OCC. The indoor LED lighting infrastructures can be transformed into positioning beacons. The camera can capture location-related information transmitted by high-frequency flickering LEDs. Rolling shutter is often used to increase the sampling rate [3], [4], [21], [22].

Communication distance is considered as a crucial performance metric in LED-based OCC systems [23], especially for vehicles and drones communications. This paper deals with the LED channel interference caused by the increase in communication distance, from the perspective of physical layer coding.

B. Hierarchical Coding

Several previous studies proposed hierarchical coding scheme to provide adaptive and scalable transmission capabilities for LED-based OCC systems. [11] utilized 2D-Haar wavelets transform to embed 3 levels of priority data into different frequency components of the traffic light LED array. The disadvantages of frequency-based hierarchical encoding had been discussed in [9]. The following work [13], [24] proposed overlay coding to deal with the limitations of hierarchical coding based on wavelet transform. They divided

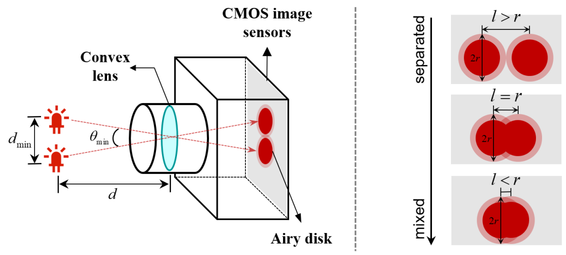

(a) Fraunhofer diffraction & Airy disk (b) Rayleigh criterion

Fig. 2. The physical principle of LED mixing. (a) optical imagery; (b) $l > r$ for separated LEDs; $l = r$ for Rayleigh criterion; $l < r$ for mixed LEDs.

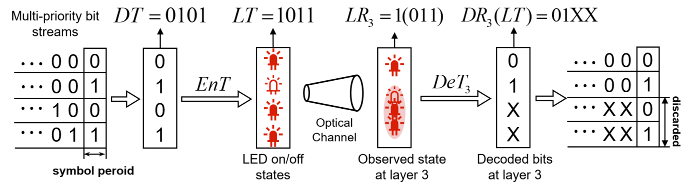

Fig. 3. Variables definition and transmission model of ONIONCODE.

the LED array into blocks of different size corresponding to different priorities or layers. Blocks with embedded bits of different layers are overlaid together to generate the overlay code. The long-distance receiver can extract the data embedded in large-size blocks, because low-frequency components can be reserved. The layered coding, Strata, proposed in [9] embedded information at multiple granularity into the same screen space. Similar as [13], Strata adopted multi-size blocks division and construct the code recursively to support various operating conditions, such as camera resolution and frame rates.

A common motivation of the existing hierarchical coding is to deal with the channel interference due to spatial aliasing. The overlay coding [13], [24] is the closest to our work. As mentioned above, the overlay code adopts a *block-based* coding, i.e., all LEDs belonging to the same block transmitted identical data bits which reduced the channel utilization. Our work designs a unique *non-block-based* hierarchical coding scheme to maximize the channel utilization.

III. BACKGROUND & PRELIMINARY

A. Rayleigh Criterion

Optical imaging instruments (such as cameras, human eyes) have limited resolving power for point light sources. Due to the Fraunhofer diffraction, the image formed by a point light source through a circular lens is not a geometric point, but a round spot with a radius r, termed as Airy disk [25] (Fig.2(a)).

As shown in Fig.2(b) , if the distance between two point light sources is rather close, the corresponding two Airy disks may partially overlap and are difficult to distinguish. The Rayleigh criterion [26] defines that an optical instrument can distinguish two point light sources, when the distance between the centers of the two Airy disks l is exactly equal to the radius r of the Airy disk. In other words, two point light sources have a minimum resolution angle given by

$$\theta_{\min} = 1.22\lambda/D \tag{1}$$

where D is the aperture diameter of the lens and λ is the wavelength of the point light source. Given that the distance between the point light sources and the optical instrument is d, the minimum distance d_{min} between two point light sources that can make them distinguishable is

$$d_{min} = d\theta_{min} \tag{2}$$

The Rayleigh criterion is the physical principle of the LED spatial mixing in Sec.III-B and the criterion can guide us to design the spatial arrangement of LEDs, so that the desired mixing phenomenon can be observed by the camera at a specific distance.

B. Formulation of LED Spatial Mixing

In the LED-based OCC system, the increase in LED-to-camera distance leads to serious LED spatial mixing. Consequently, the receiver cannot distinguish the luminance of adjacent LEDs and fails to decode. This section formulates the LED spatial mixing which is the preliminary of the ONIONCODE scheme. For the ease of understanding, we first give the ONIONCODE transmission model, the important variables introduced in this section are labeled in the Fig.3.

1) Non-uniform LED arrangement and mix-LED: We assume that L LEDs are non-uniformly arranged on a plane. *Non-uniform*" means that the interval between any two LEDs is not equal and this assumption will be further discussed in Sec.VII. Due to the non-uniform arrangement, the LEDs mix one after another in a specific order, as the LED-to-camera distance increases. As shown in Fig.1(a), the interval between LED-3 and LED-4 is the closest, so they are mixed first at layer 2. Here, we introduce the concept of *layer* based on the observed mixing status. A camera at layer $k > 1$ can capture a frame containing $L - k$ *independent-LED* and a *mix-LED*, which is mixed by k LEDs and we denote it as L_k. From the perspective of MIMO communication, both independent-LED and mix-LED can be viewed as a communication channel, which we call *independent-LED channel* and *mix-LED channel* in this paper. Besides, the definition of "mixing" is that the two farthest apart of the k LEDs just meet the Rayleigh criterion, i.e., these k LEDs cannot be separated spatially.

2) LED State Space: We define the *LED state space* for each layer, which is the foundation of the ONIONCODE derivative. Fig.4 shows the LED state space of layer 3. For simplicity, we denote the transmitter's L-LEDs on/off states within a symbol period as $LT = l_1 l_2 \cdots l_i \cdots l_L, l_i \in \{0, 1\}$ (0 for off, 1 for on). For example, the 2-th column of Fig.4 means that when $LT \in \{0001, 0010, 0100\}$, the camera can distinguish an independent off-LED and a mix-LED L_3 with 1 LED on. The mix-LED is indicated by the parentheses.

We define a *state*, LR_k^i, of layer k as a group of LT that can be distinguished by the receiver. For example, the LR_3^2 in Fig.4 contains 3 LT which can not be distinguished by the camera due to spatial mixing. Obviously, the k-th layer contains $(k + 1) \times 2^{L-k}$ states. As mentioned before, a state LR_k^i contains C_k^t indistinguishable LT, which are termed as *sub-state* of LR_k^i, where t is the number of on-LEDs in L_k.

LR_3^i	1	2	3	4	5	6	7	8
Layer 3	0(000)	0(001) 0(010) 0(100)	0(011) 0(101) 0(110)	0(111)	1(000)	1(001) 1(010) 1(100)	1(011) 1(101) 1(110)	1(111)

Fig. 4. LED state space of layer 3

All states $LR_k^i, k = 1, 2, \cdots, L; i = 1, 2, \cdots, (k+1) \times 2^{L-k}$ constitute the state space of the L non-uniform LEDs.

C. Formulation of Multi-Priority Transmission

Denote the data bits transmitted by L-LEDs within a symbol period as $DT = d_1 d_2 \cdots d_i \cdots d_L, d_i \in \{0, 1\}$. DT is modulated to LT at the transmitter, and the bits decoded from LT at a k-th layer receiver are $DR_k(LT) = r_1 r_2 \cdots r_i \cdots r_L, r_i \in \{0, 1, \mathrm{X}\}$, where X indicates that the corresponding bit will be discarded defined as *discarded bit*. The design goals of layered coding can be expressed as

$$DR_1(LT) = DT \tag{3}$$

$$DR_i(LT) \subset DR_j(LT), i > j \tag{4}$$

Eq. 3 indicates that the camera at layer 1 can decode all the bits of DT. As the LED-to-camera increases, more bits will be discarded and Eq. 4 means that the lower layer can reserve more data bits than the higher layer. For example, the 4-LEDs transmitter sends bits $DT = 0011$, then the bits received by layer $1\sim4$ are $0001, 000\mathrm{X}, 00\mathrm{XX}, 0\mathrm{XXX}$, as shown in Fig .1(b). In summary, the proposed OnionCode assigns different *priorities* to each bit of DT. As the LED-to-camera distance increases, the low-priority bits will be discarded first, and the highest-priority bit can be reserved.

D. The Transmission Model of OnionCode

The core modules of OnionCode include an *encoding table* EnT for the transmitter and L *decoding tables* $DeT_i, i \in [1, L]$ for the receiver at each layer. EnT is defined as the mapping from DT to LT and DnT_k is defined as the mapping from LR_k to $DR_k(LT)$, the data transmission can be modeled as Eq. 5 and the related definition is shown in Fig.3.

$$DT \overset{EnT}{\longmapsto} LT \overset{OpticalChannel}{\Longrightarrow} LR_k^i \overset{DnT_k}{\longmapsto} DR_k(LT) \tag{5}$$

IV. OnionCode scheme

Before giving a specific coding scheme, this section first introduces the overall design goal of layered coding. We takes $L = 4$ as an example to explain the derivation process of the encoding/decoding table, and then gives a proof of generalized derivation. Finally, we summarize the two key insights of OnionCode.

A. Decoding Table Derivation

The derivation is carried out in an *iterative* manner, starting from the LED state space of the highest layer (layer 4).

Fig. 5(a) is a feasible decoding table for layer 4. For example, the 2-nd column means that the state LR_4^2 is *mapped* to demodulated bits $DR_4(LT) = 0\mathrm{XXX}$, where $LT \in \{0001, 0010, 0100, 1000\}$. As mentioned in Sec.III-C, layer 4 discards 3 data bits, that is to reserve 0XXX and 1XXX. 3 discarded bits XXX contains $2^3 = 8$ possible LEDs on/off states, from 000 to 111. We select LR_4^1, LR_4^3 and map them to 0XXX, because the total sub-states of LR_4^1 and LR_4^3 is 8, which is enough to accommodate 8 possible on/off states. Similarly, the state $LR_4^i, i = 0, 2, 4$ are mapped to 1XXX.

LR_4^i	0	1	2	3	4
Layer 4	(0000)	(0001) (0010) (0100) (1000)	(0011) (0101) (0110) (1001) (1010) (1100)	(0111) (1011) (1101) (1110)	(1111)
$DR_4(LT)$	1XXX	**0XXX**	1XXX	**0XXX**	1XXX

(a) Decoding table of layer 4.

LR_3^i	···	1	3	4	5	···
Layer 3	···	0(001) 0(010) 0(100)	0(111)	1(000)	1(011) 1(101) 1(110)	···
$DR_3(LT)$		**00XX**	**00XX**	01XX	01XX	

(b) Decoding table of layer 3.

LR_2^i	···	1	3	5	···
Layer 2	···	00(01) 00(10)	01(00)	01(11)	···
$DR_2(LT)$		**000X**	001X	001X	

(c) Decoding table of layer 2.

LR_3^i	···	1	2	···
Layer 1	···	0001	0010	···
$DR_1(LT)$		**0000**	0001	

(d) Decoding table of layer 1.

Fig. 5. Feasible decoding table from layer 4 to layer 1.

At layer 3, we focus on the 8 sub-states (blue figures in Fig.5(a)) that are mapped to 0XXX at layer 4, these sub-states are rearranged to states $LR_4^i, i = 1, 3, 4, 5$ at layer 3. Under this condition, we only need to consider the mapping of 00XX and 01XX. Similarly, 00XX needs 4 sub-states to accommodate $2^2 = 4$ possible on/off states contributed by 2 discarded bits. Hence, we map LR_3^1, LR_3^3 to 00XX, marked in blue in Fig.5(b). The mapping of 000X at layer 2 and 0000 at layer 1 follows the same process, as shown in Fig.5(c) and (d). For simplicity, we only demonstrate part of the decoding table of each layer.

B. Conclusion from the Decoding Table Derivation

From the derivation above, we come into the following 3 conclusions:

- A key insight is that the $(k-1)$ discarded bits in $DR_k(LT)$ determines which states should be mapped to $DR_k(LT)$. Specifically, the states $\{LR_k^i\}$ mapped to $DR_k(LT)$ should meet the Eq. 6, where $N(LR_k^i)$ is the number of sub-states of state LR_k^i.

$$\sum\nolimits_i N\left(LR_k^i\right) = 2^{k-1} \tag{6}$$

- Fig.5(a)-(d) only show the mapping of 0XXX, 00XX, 000X, 0000 at the corresponding layers. Obviously, the derivation process is *iterative* and *symmetric*, which means the mapping of bit "1" could follow the same process at each layer.

- To obtain the encoding table EnT of the transmitter, we only need to *reverse* DeT_1, the decoding table of layer 1. For example, If $DT = 0000$ (1-st column in Fig.5(d)), the LT should be 0001. The LEDs states observed by the cameras at the layer 1∼4 are 0001, 00(01), 0(001) and (0001), and the decoded bits are 0000, 000X, 00XX and 0XXX respectively.

C. Generalized Derivation

In this section, we introduce the decoding table derivation in a general manner.

1) STEP1: The derivation of DeT_L: The number of discarded bits of Layer L is $L-1$, hence, all states $\{LR_L^i, i = 1, \cdots, (k-1) \times 2^k\}$ should be partationed into 2 subsets and each subset should meet the Eq. 6. We define the *state vector* of the layer L as

$$SV_L = (C_L^0, C_L^1, \cdots, C_L^t, \cdots, C_L^{L-1}, C_L^L) \tag{7}$$

The elements of SV_L is ordered and equal to the sub-states number of corresponding state. t is the number of on-LEDs in L_k of LR_L^i and C is the combination operation. For example, $SV_L = (1, 4, 6, 4, 1), L = 4$.

For the combination numbers in SV_L, the following equation is established

$$C_L^0 + C_L^2 + C_L^4 + \cdots = C_L^1 + C_L^3 + C_L^5 + \cdots = 2^{L-1} \tag{8}$$

Eq. 8 indicates that the elements of SV_L can be partitioned into 2 *equal-sum* subsets, corresponding to the odd and even terms. Hence, the odd-terms SV_L^{odd} can be mapped to bits $B_L^0 = 0XX\cdots X$ and even-terms SV_L^{even} to $B_L^1 = 1XX\cdots X$, as Fig.5(a) shows.

2) STEP2: The derivation of DeT_{L-1}: Similarly, we focus on the SV_L^{odd} mapped to $0XX\cdots X$ at layer L in *STEP 1*. For combination C_L^k, the following equation is established

$$C_L^k = C_{L-1}^k + C_{L-1}^{k-1} \tag{9}$$

According to Eq. 9, the odd-terms SV_L^{odd} at layer L are *rearranged* to $SV_{L-1} = \{C_{L-1}^0, C_{L-1}^1, \cdots, C_{L-1}^{L-1}\}$ at layer $L-1$, as Fig.5(a) to (b) shows. From Eq. 7 and 8, SV_{L-1} can be partitioned into odd and even terms and mapped to $B_{L-1}^0 = 00X\cdots X$ and $B_{L-1}^1 = 01X\cdots X$ respectively.

3) STEP3: The derivation of DeT_k: Obviously, the *STEP 2* is iterable thanks to Eq. 8 and 9, and can be generalized to any layer. By reversing the DeT_1, the encoding table EnT can be obtained.

The generalized algorithm of the encoding/decoding table generation is shown in **Algorithm 1**. For further explanation, *line 12* means adding the two mapping $(x, y) : x \mapsto y$ to the table DeT_k and *line 6* means reversing the mapping of DeT_1 to obtain EnT.

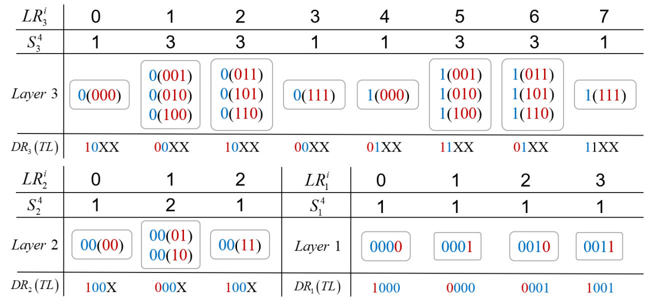

(a) Correspondence between LED channel and decoded data bits. Red for the mix-LED channel and blue for the independent-LED channel.

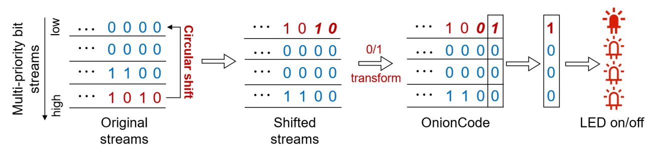

(b) Circular shift of ONIONCODE encoding process.

Fig. 6. Two deep insights of ONIONCODE.

D. Deep insight of ONIONCODE & Decoding Error Analysis

Without layered coding, the decoding of L parallel LED channels conducts independently, hence, bit errors of different channels are independent. Layered coding decodes parallel channels in a coupled manner, but in fact, it can be proved that bit errors are still independent. To explain the error independence of layered coding, we deeply analyze the principle of layered coding from the perspective of *LEDs state space*. As shown in Fig.4, the states LR_k^i of layer k are arranged in a specific order, according to the smallest sub-state of LR_k^i. The "smallest" here means that the sub-state has the smallest binary value Under the specific states order, we can simply

---

Algorithm 1: Encoding/decoding table generation

input : The number of LEDs: L
output: A encoding table EnT of layer 1 and L decoding table $DeT_i, i = 1, 2, \cdots, L$

1 **Function:** EnT, $\{DeT_i\}$ = *Main*(L);
2 $\quad SV_L = \{C_L^0, C_L^1, \cdots, C_L^L\}$;
3 $\quad B_L = XX\cdots X$;
4 $\quad EnT = \emptyset$, $DeT_i = \emptyset, i = 1, 2, \cdots, L$;
5 $\quad$ *Mapping*(SV_L, B_L);
6 $\quad EnT$ = *Reverse*(DeT_1);
7 $\quad$ **return** EnT, $\{DeT_i\}$;

8 **Function:** *Mapping*(SV_k, B_k);
9 $\quad$ Convert B_k to B_{k-1}^0 and B_{k-1}^1;
10 $\quad$ Rearrange SV_k to SV_{k-1} (Eq. 9);
11 $\quad$ Partition SV_{k-1} into SV_{k-1}^{odd} and SV_{k-1}^{even}(Eq. 8);
12 $\quad DeT_k += \{(SV_{k-1}^{odd}, B_{k-1}^0), (SV_{k-1}^{even}, B_{k-1}^1)\}$;
13 $\quad$ **if** $k > 1$ **then**
14 $\quad\quad$ *Mapping*(SV_{k-1}^{odd}, B_{k-1}^0);
15 $\quad\quad$ *Mapping*(SV_{k-1}^{even}, B_{k-1}^1);

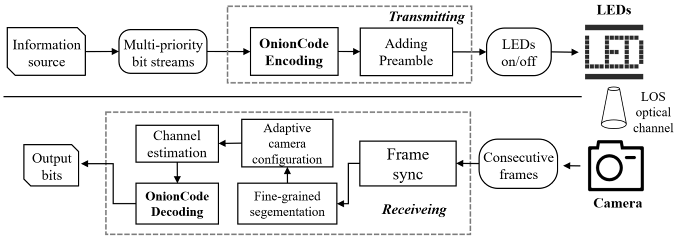

Fig. 7. Architecture of ONIONCODE prototype.

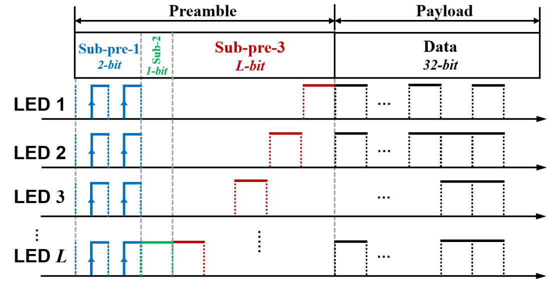

Fig. 8. Frame structure of ONIONCODE.

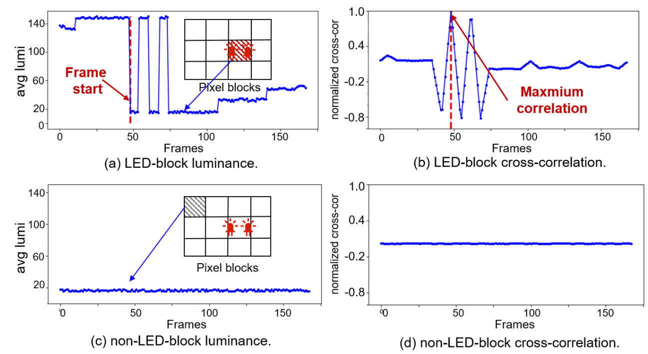

Fig. 9. Process of frame synchronization. A frame is divided into several blocks, and only the blocks containing flickering LEDs can be detected.

use the state vector SV_k^L to represent the states of layer k:

$$S_k^L = SV_k^L \otimes 2^{L-k} \tag{10}$$

where "$\otimes 2^{L-k}$" means concatenating 2^{L-k} SV_k^L together, for example, $S_4^3 = (1,3,3,1) \otimes 2 = ((1,3,3,1),(1,3,3,1))$. Eq. 9 is the root of the establishment of Eq. 10.

According to Eq. 8, the SV_k^L can be partitioned into two equal-sum subsets to encode 1 bit which can be decoded from the mix-LED channel, and the other $L-k$ bits can be decoded from the $L-k$ independent-LED channels, because SV_k^L is repeated 2^{L-k} times. The bits decoded from the mix-LED channel and from $L-k$ independent-LED channels are marked as red and blue respectively in Fig.6(a) to illustrate the above correspondence at each layer.

Two deep insights can be obtained from Fig.6(a):

- At each layer, only 1 bit is encoded in the mix-LED channel. In this sense, the capacity of the mix-LED channel and the independent LED channel are equal. This insight can be generalized to the case where there exist multiple mix-LED channels.
- The encoding process of layer 1 shows that, ONIONCODE essentially cyclically shifts L bit streams and then performs 0/1 transformation on the highest priority bit according to the encoding table, as shown in Fig.6(b). Hence, the bit errors of different LED channels are *independent*.

V. ONIONCODE OCC PROTOTYPE

A. System Overview

We established an *proof-of-concept* OCC system enhanced by the proposed layered coding. Fig.7 illustrates the system architecture, comprising of multiple LEDs as the transmitter and a camera as the receiver.

- At the transmitter, the multi-priority bit streams generated by the information source are first mapped to ONIONCODE according to the encoding table and framed with a customized preamble. Then, the bit streams are converted to the LEDs on/off states for transmission.
- At the receiver, the camera first performs frame synchronization in the captured frames and the fine-grained segmentation separate LED channels spatially. Then, the adaptive camera configuration adjusts the optimal exposure parameters for accurate channel estimation. Finally, the ONIONCODE can be decoded according to the result of channel estimation.

B. Transmitter Design

The transmitter sends the multi-priority bit streams through parallel optical channels and Fig.8 illustrates the frame structure of a single LED channel. Each frame contains 32 data bits framed with a customized preamble composed of 3 sub preambles. The sub-preamble-1 is prepended for *frame synchronization* and *fine-grained LED segmentation*. The sub-preamble-2 and 3 are designed for *camera configuration* and *optical channel estimation* respectively. We adopt the baseband transmission method using NRZ line code which is simple but sufficient to prove the effectiveness of ONIONCODE.

C. Receiver Design

1) Frame Synchronization: Enlightened by [27], we design the sub-preamble-1 consisting of 2 repeated Manchester bits for frame synchronization and fine-grained LED segmentation. In this section, we focus on the spatial and temporal frame synchronization based on cross-correlation search.

As shown in Fig.9, we divide a frame into pixel blocks of equal size. For each block, a filter matching with the sub-preamble-1 is used for cross-correlation calculation. x blocks with the highest cross-correlation value are extracted, which indicate the coarse positions of the LEDs. Then, we combine the x blocks together, and perform cross-correlation calculation again. Finally, the preamble start can be identified according to the maximum cross-correlation. The combination of blocks is to cope with the small movement of the camera or LED. The size of the pixel block and x depend on the LEDs arrangement and camera's resolution. In our experiment, x is set to 5 and block size to 20×20.

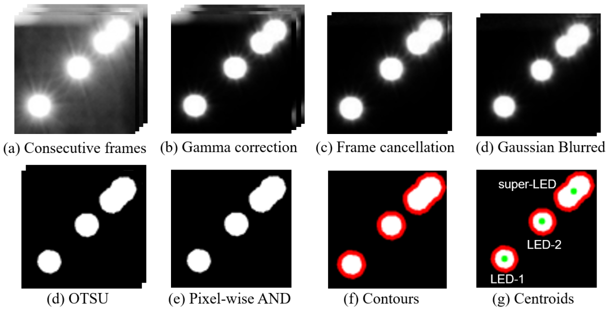

(a) Consecutive frames (b) Gamma correction (c) Frame cancellation (d) Gaussian Blurred

(d) OTSU (e) Pixel-wise AND (f) Contours (g) Centroids

Fig. 10. Pipeline of fine-grained LED segmentation.

2) Fine-grained LED Segmentation: Following the frame synchronization, we continue to use sub-preamble-1 to segment the LEDs at the pixel level. Although the frame synchronization has given a coarse LED position, fine-grained LED segmentation is still necessary to: 1) further separate the background noise and improve the SNR; 2) measure the number of aliased LEDs and determine the decoding table to be used.

We combine the frame-level cancellation [5] and the boundary detection algorithm [3] together. As shown in Fig.10(a)-(g), we extractadap consecutive frames with the LEDs alternating between ON and OFF during the sub-preamle-1 and *gamma correction*($\gamma > 1$) is used to redistribute the gray values. In our experiment, gamma correction can effectively reduce the impact of ambient reflected light. For each frame generated by consecutive subtraction, gaussian blurring further suppresses background noise and OTSU's method [28] binarizes the image adaptively. The obtained binary frames are combined through pixel-wise "AND" in order to deal with the moving background objects. Finally, we find the contours [29]adap and centers for each LED as Luxapose [3] and identify each LED according to center-to-center distance.

3) Adaptive Camera Configuration: The camera's exposure parameters have a great impact on the SNR of the mix-LED channel as shown in Fig.11(a). We introduce the concept of *average luminance* to explain the effect of exposure parameters. The average luminance of mix-LED L_k is defined as Eq. 11, where $S(L_k)$ is the pixel area occupied by the mix-LED (area within the red contour in Fig.10(g)), and x is the number of on-LEDs in L_k. $Lumi(L_k(x))$ is the the total luminance of all pixels in $S(L_k)$.

$$Avg(L_k(x)) = Lumi(L_k(x))/S(L_k) \tag{11}$$

As shown in Fig .11(b1), the auto exposure makes pixel luminance close to the maximum, as a result, the LED spatial overlapping makes $Avg(L_k(x))$ unevenly spaced between 0-255, leading to confusing luminance level as x increases. On the other hand, low exposure also makes the decoding of mix-LED error-prone, as shown in Fig .11(b2), because the $Avg(L_k(x))$ distribute closely to each other. The impact of low exposure can also be observed in Fig .11(a).

Therefore, we design an adaptive camera configuration mechanism for optimal exposure as shown in Fig. 11(b3). During sub-preamble-2, only one LED is lit, enabling the camera to measure the $Avg(L_k(1))$, and adjust the exposure parameters to make Eq. 12 established.

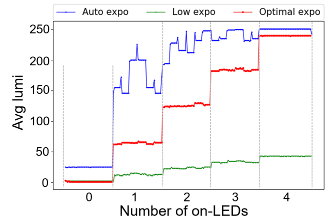

(a) Average luminance under automatic exposure, low exposure and optimal exposure.

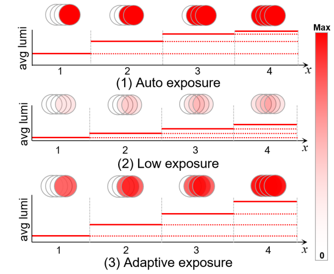

(b) The impact of exposure on the average luminance of mix-LED.

Fig. 11. Basis for adaptive camera configuration.

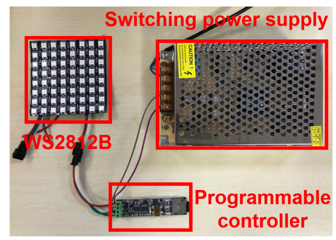

(a) LED drive circuit.

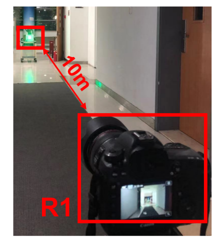

(b) Receiver at layer 1.

Fig. 12. Prototype of ONIONCODE.

$$Avg(L_k(1)) \approx 255/k \tag{12}$$

Eq. 12 keeps the $Avg(L_k(x))$ evenly distributed between 0-255. In practice, we set a high shutter speed and a small aperture in advance, and adjust the ISO according to the pre-calibrated ISO-luminance curve. Noting that the exposure adjustment has a minor impact on frame synchronization and LED segmentation, because all the LEDs flickers simultaneously during sub-preamble-1. We verify this conclusion in Sec.V-C3.

4) Optical Channel Estimation: For independent-LED, the channel estimation can be easily achieved by transmitting 0/1 symbols. But for the mix-LED L_k, up to 2^k symbols are needed to achieve complete channel estimation, which is a huge communication overhead, and k is various at different layers. Therefore, we design a low-overhead and layer-uniform channel estimation method (sub-preamble-3) for the mix-LED channel.

In sub-preamble-3, all the LEDs are lit sequentially, enabling the receiver at layer k to measure the $Avg(L_k(1))$ of the mix-LED. We predict the $Avg(L_k(x))$ by linearly combining the $Avg(L_k(1))$ and $Lumi(L_k(0))$ (background noise) as Eq. 13. This estimation holds under the condition of Eq. 12 and superposition principle of incoherent light [30].

$$\begin{aligned}\widehat{Avg}(L_k(x)) = \;& x \times Avg(L_k(1)) \\ & - (x-1) \times Lumi(L_k(0))\end{aligned} \tag{13}$$

In fact, the linear prediction in Eq. 13 is overestimated $\widehat{Avg}(L_k(x)) > Avg(L_k(x))$. As the number of on-LEDs x increases, the voltage of the parallel LEDs will decrease, weakening the luminance of each on-LED. Fortunately, we can pre-measure the voltage drop of the LED circuit at various x

and correct the $Avg(L_k(1))$ by multiplying a correction factor $V(x) < 1$, based on the non-linear relationship between LED voltage and luminance [31].

VI. Evaluation

A. System Prototype

As shown in Fig.V-C3, we prototype the OnionCode using WS2812B [32] intelligent control LED (5V, 16W) as the transmitter. The WS2812B can be controlled by a programmable controller which is powered by a 5V,12A switching power supply.

We tested OnionCode with various types of receivers, including Canon EOS 5D Mark IV [33] (1080p, 50Hz), Zenmuse H20 [34] (1080p, 30Hz), and iPhone X [35] 1080p, 50Hz). We evaluated the performance of OnionCode in one-to-many communication scenario where 4 receivers are placed at 10m, 20m, 30m, and 40m (denoted as R_1, R_2, R_3, and R_4 in the following evaluation) from the transmitter, corresponding to layer 1-4 receivers. Note that we used 4 LEDs and 4-layer priority for most evaluation but OnionCode can be easily scaled as shown in Sec. IV-C.

B. Micro Benchmark

1) Preamble Detection: We start by evaluating the robustness of the frame synchronization and segmentation scheme. We define frame detection accuracy as the ratio of frames that are correctly detected in both time (synchronization) and space (segmentation). Fig. 13(a) shows the detection accuracy under various light condition. "indoor" represents the experiments done in ordinary office environment with light on; "outdoor" represents the experiments done outdoor at noon with strong sunlight. We can see that the synchronous flickering LED can be effectively detected by cross-correlation searching, so the detection accuracy achieves 99.4% and 99.3% in both scenarios. We then evaluate the impact of movement. Fig. 13(b) shows the detection accuracy while the receivers are placed still on a tripod, held by a hand with slight shaking. We also tested the detection with static indoor office background ("static") and moving pedestrian ("moving"). We can see that the detection accuracy can reach 98.6% even held by hand and with moving pedestrian, because the matched filter and cross-correlation can filter moving background objects, and block-based operations can tolerate small-range LED movements.

2) Camera Configuration: As shown in Sec. V-C3, we design the preamble so that the receivers can adaptively configure the camera exposure parameter to ensure strong SNRs. We compared the proposed adaptive camera configuration scheme with those using camera's built-in auto-exposure or low exposure and repeated the test under different outdoor ambient light. In order to highlight the advantage of adaptive exposure, we set a mix-LED mixed by 9 LEDs (3×3 arrangement) and measured the bit correct rate (BCR) of the mix-LED channel. The results is reported in Fig. 14(a).

We can see that the proposed adaptive scheme outperforms built-in auto-exposure and low exposure scheme by 268.0% and 24.3%, respectively. Fig. 14(b) demonstrated the observed average luminance distribution, the adaptive configuration can provide a higher error tolerance.

3) Channel Estimation: In Sec. V-C4, we design the sub-preamble-3 to predict the measured luminance of mix-LED, so we can reduce the length of preamble. In this subsection, we evaluate the effectiveness of the proposed scheme by comparing the luminance measured and predicted by various schemes. Fig. 15 shows the results. "linear" represents the prediction scheme which assume the luminance is linearly proportional to the number of on-LEDs.

We calculate the mean square error (MSE) of the predicted and measured luminance at various on-led numbers. The MSE is reported in Table.I. We can see that the proposed scheme outperforms "linear" and reduces average MSE by 94.3%.

C. Overall Performance

1) System Throughput: We compare the proposed OnionCode with the state-of-the-art layered coding (overlay coding [13]). The overlay coding uses 4 LEDs and follows the same frame structure as OnionCode. In addition, a reference group without a hierarchical coding scheme ("w/o") was set up for comparison. Fig. 16 shows the results. To make the comparison more intuitive, we normalize the throughput by making R_1 (i.e., the layer-1 receiver that can decode all information from the encoded data) 1. We can then make the following observations. First, the throughput of R_1 using OnionCode is as high as that in the reference group ("w/o"). In contrast, the throughput of R_1 using overlay coding is 25.5% lower. It implies that OnionCode does not need to sacrifice the channel capacity of R_1 to achieve multi-priority transmission; however, overlay coding requires the injection of redundant bits, so the throughput becomes lower. Second, when LED space mixing occurs (i.e., in R_2 to R_4), the conventional coding scheme ("w/o") fails and the throughput drops to 0. In OnionCode, R_2 to R_4 still decodes 75.5%, 51.2% and 24.8% of the transmitted data. Overlay coding also allows R_2 to R_4 to decode some of the data; however, since it only supports 2-layer priority, R_2 to R_4 has the same throughput. Finally, OnionCode greatly improves the overall throughput by a factor of 167% compared to overlay coding.

2) Robustness of OnionCode: We further evaluate the throughput of OnionCode under various environment factors and hardware conditions. For comparison, we set up a reference group with indoor static background and the camera is held by tripod.

Receiver Hardware. Fig. 17(b) reports the normalized throughput of the OnionCode using COTS drone-mounted and mobile phone cameras as the receiver. The throughput of the 3 receivers approaches their theoretical value, which reflects the robustness of the OnionCode prototype to the

TABLE I
MSE comparison between linear prediction and our method

Method	1	2	3	4	5	6	7	8	9	Avg
Linear	0.44	4.13	8.42	13.96	21.82	29.55	35.65	43.14	51.58	23.19
Ours	0.44	0.52	0.83	0.76	1.06	1.35	1.31	4.27	1.32	**1.32**

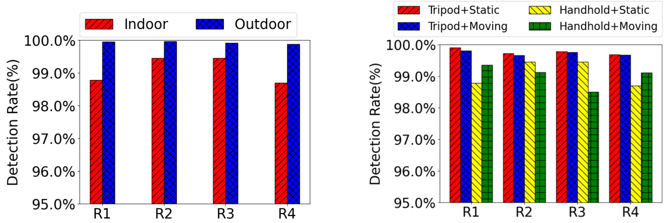

(a) Various ambient light.

(b) Movement.

Fig. 13. Preamble detection rate under various environment factors.

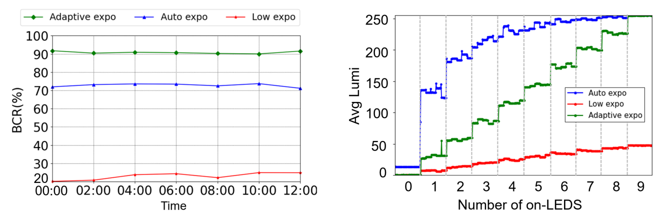

(a) BCR of 3 exposure schemes.

(b) Luminance distribution.

Fig. 14. Evaluation of the proposed adaptive camera configuration.

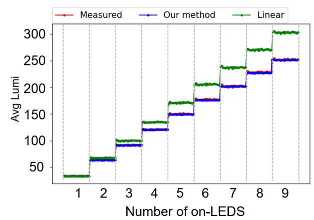

Fig. 15. mix-LED channel estimation using linear prediction and our method.

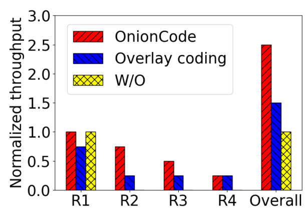

Fig. 16. Performance comparison between ONIONCODE, Overlay Coding [13], and without hierarchical coding ("w/o").

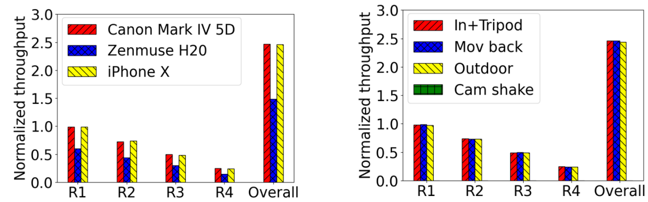

(a) Various cameras.

(b) Various environment factors.

Fig. 17. Robustness of ONIONCODE. R_1 to R_4 represents the receivers at various distances and decode up to layer-1 to layer-4 messages, respectively.

hardware conditions. Here, we use the Canon camera at layer 1 as the reference group for normalization.

Environmental Factors. Fig. 17(a) shows that ONIONCODE is robust against ambient light and moving pedestrian, keeping the same throughput as the reference group. Specifically, the adaptive camera configuration can ensure the strong SNR under various ambient light, and the frame synchronization based on cross-correlation filters out the moving objects. However, the current ONIONCODE prototype nearly fails as the camera is held in hand. This limitation originates from the fine-grained LED segmentation in Sec.V-C2. The segmentation is only performed during sub-preamble-1, and if the camera shakes or the LED moves away later, the target LED will be lost. Therefore, the following channel estimation and decoding are meaningless.

VII. DISCUSSION

A. Potential Application

OCC is considered a promising communication method for quadrotor drones communications (OCC for drones) [18], [36] thanks to the high-resolution drone-mounted cameras. Compared with the existing "one drone-to-one controller" communication using radio frequency band, OCC can provide multilateral communication between a camera and multiple drones. In addition, mobile phones can also be used as receivers, so that information can be transmitted to non-UAV pilots via optical channels. This advantage is promising for post-disaster monitoring [16], [37]. In this scenario, the coordinates of the trapped person can be high-priority data, and the image of the trapped scene can be used as low-priority data. Multi-priority hierarchical transmission scheme of ONIONCODE ensures that high-priority data can be received by remote receivers. In other words, ONIONCODE can be regarded as a software-method to increase the communication range of OCC for drones.

B. Limitations & Future work

Non-uniform LEDs Arrangement. The non-uniform distribution of L LEDs is designed to generate L priority layers, because the number of mixed LEDs consecutively increases from 1 to L. Non-uniform LED arrangement is common for OCC in practical applications. For example, when we reuse LEDs on drones, traffic light, light in office environment, etc to enable side channel communications for V2X and light positioning applications, the light placement is not controlled and therefore usually non-uniform. Moreover, even for uniformly arranged LEDs, ONIONCODE can also be applied since the corresponding layers disappear without affecting the decoding of other layers. For example, if the LED 2, 3, 4 in Fig. 1(a) are uniformly arranged, the layer 1, 3, 4 are not affected, even if layer 2 disappears. On the other hand, the number of layers is actually determined by the application. Most application scenarios do not need all L layers, hence, the size of LED transmitter can be greatly reduced. In addition, optimization methods can be utilized to maximize the space utilization, which is also a future direction of ONIONCODE.

Error Control. The application of error control mechanisms, such as forward error correction (FEC) [38] and retransmission, can further improve the transmission robustness of ONIONCODE and achieve higher throughput in noisy channels. However, in this work, we decided to leave the error control mechanisms to a higher layer of the communication protocol and focus on the design of ONIONCODE itself, aiming at achieving higher coding efficiency and understanding its own performance in the absence of error control.

VIII. CONCLUSION

In this paper, we present a multi-priority hierarchical coding for optical camera communication, named as ONIONCODE. The systematic analysis of LED channel aliasing provides a prerequisite for us to fully exploit the capacity of the aliasing channel. The proposed ONIONCODE allows the receiver to dynamically discard low-priority data according to the measured optical channel states and the highest priority data can be reserved by the long-distance receiver. We prototype the ONIONCODE using COTS digital cameras and commonly-used LED. A variety of communication mechanisms are devised, including frame synchronization, fine-grained LED segmentation, adaptive camera configuration and aliasing channel estimation, to achieve low-overhead and noise-robust communication functions. Experiment results demonstrate the effectiveness of ONIONCODE. Compared with the existing block-based hierarchical coding scheme, ONIONCODE can maximize channel utilization.

ACKNOWLEDGEMENT

This work is supported in part by National Key R&D Program of China (2018YFB2101102), NSFC (U1736207, 62072306) and Program of Shanghai Academic Research Leader (20XD1402100).

REFERENCES

[1] Nasir Saeed, Shuaishuai Guo, Ki-Hong Park, Tareq Y Al-Naffouri, and Mohamed-Slim Alouini. Optical camera communications: Survey, use cases, challenges, and future trends. *Physical Communication*, 37:100900, 2019.

[2] Liqun Li, Pan Hu, Chunyi Peng, Guobin Shen, and Feng Zhao. Epsilon: A visible light based positioning system. In *11th {USENIX} Symposium on Networked Systems Design and Implementation ({NSDI} 14)*, pages 331–343, 2014.

[3] Ye-Sheng Kuo, Pat Pannuto, Ko-Jen Hsiao, and Prabal Dutta. Luxapose: Indoor positioning with mobile phones and visible light. In *Proceedings of the 20th annual international conference on Mobile computing and networking*, pages 447–458, 2014.

[4] Niranjini Rajagopal, Patrick Lazik, and Anthony Rowe. Visual light landmarks for mobile devices. In *IPSN-14 proceedings of the 13th international symposium on information processing in sensor networks*, pages 249–260. IEEE, 2014.

[5] Samuel David Perli, Nabeel Ahmed, and Dina Katabi. Pixnet: Interference-free wireless links using lcd-camera pairs. In *Proceedings of the sixteenth annual international conference on Mobile computing and networking*, pages 137–148, 2010.

[6] Tian Hao, Ruogu Zhou, and Guoliang Xing. Cobra: Color barcode streaming for smartphone systems. In *Proceedings of the 10th international conference on Mobile systems, applications, and services*, pages 85–98, 2012.

[7] Wenjun Hu, Hao Gu, and Qifan Pu. Lightsync: Unsynchronized visual communication over screen-camera links. In *Proceedings of the 19th annual international conference on Mobile computing & networking*, pages 15–26, 2013.

[8] Hui-Yu Lee, Hao-Min Lin, Yu-Lin Wei, Hsin-I Wu, Hsin-Mu Tsai, and Kate Ching-Ju Lin. Rollinglight: Enabling line-of-sight light-to-camera communications. In *Proceedings of the 13th Annual International Conference on Mobile Systems, Applications, and Services*, pages 167–180, 2015.

[9] Wenjun Hu, Jingshu Mao, Zihui Huang, Yiqing Xue, Junfeng She, Kaigui Bian, and Guobin Shen. Strata: Layered coding for scalable visual communication. In *Proceedings of the 20th annual international conference on Mobile computing and networking*, pages 79–90, 2014.

[10] Hao Pan, Yi-Chao Chen, Lanqing Yang, Guangtao Xue, Chuang-Wen You, and Xiaoyu Ji. mqrcode: Secure qr code using nonlinearity of spatial frequency in light. In *The 25th Annual International Conference on Mobile Computing and Networking*, pages 1–18, 2019.

[11] Shintaro Arai, Shohei Mase, Takaya Yamazato, Tomohiro Endo, Toshiaki Fujii, Masayuki Tanimoto, Kiyosumi Kidono, Yoshikatsu Kimura, and Yoshiki Ninomiya. Experimental on hierarchical transmission scheme for visible light communication using led traffic light and high-speed camera. In *2007 IEEE 66th Vehicular Technology Conference*, pages 2174–2178. IEEE, 2007.

[12] Takaya Yamazato, Isamu Takai, Hiraku Okada, Toshiaki Fujii, Tomohiro Yendo, Shintaro Arai, Michinori Andoh, Tomohisa Harada, Keita Yasutomi, Keiichiro Kagawa, et al. Image-sensor-based visible light communication for automotive applications. *IEEE Communications Magazine*, 52(7):88–97, 2014.

[13] Sayaka Nishimoto, Tom Nagura, Takaya Yamazato, Tomohiro Yendo, Toshiaki Fujii, Hiraku Okada, and Shintaro Arai. Overlay coding for road-to-vehicle visible light communication using led array and high-speed camera. In *2011 14th International IEEE Conference on Intelligent Transportation Systems (ITSC)*, pages 1704–1709. IEEE, 2011.

[14] Shintaro Arai, Yasutaka Shiraki, Takaya Yamazato, Hiraku Okada, Toshiaki Fujii, and Tomohiro Yendo. Multiple led arrays acquisition for image-sensor-based i2v-vlc using block matching. In *2014 IEEE 11th Consumer Communications and Networking Conference (CCNC)*, pages 605–610. IEEE, 2014.

[15] Shun-Hsiang You, Shih-Hao Chang, Hao-Min Lin, and Hsin-Mu Tsai. Visible light communications for scooter safety. In *Proceeding of the 11th annual international conference on Mobile systems, applications, and services*, pages 509–510, 2013.

[16] Hiroki Takano, Daisuke Hisano, Mutsuki Nakahara, Kosuke Suzuoki, Kazuki Maruta, Yukito Onodera, Ryo Yaegashi, and Yu Nakayama. Visible light communication on led-equipped drone and object-detecting camera for post-disaster monitoring. In *2021 IEEE 93rd Vehicular Technology Conference (VTC2021-Spring)*, pages 1–5. IEEE, 2021.

[17] Bhawana Chhaglani, Abhay Sheel Anand, Nakul Garg, and Ashwin Ashok. Evaluating led-camera communication for drones. In *Proceedings of the Workshop on Light Up the IoT*, pages 18–23, 2020.

[18] Ashwin Ashok. Position: Dronevlc: visible light communication for aerial vehicular networking. In *Proceedings of the 4th ACM Workshop on Visible Light Communication Systems*, pages 29–30, 2017.

[19] Chun-Yu Chen, Bo-Yao Lin, Junding Wang, and Kang G Shin. Keep others from peeking at your mobile device screen! In *The 25th Annual International Conference on Mobile Computing and Networking*, pages 1–16, 2019.

[20] Shivani Teli, Willy Anugrah Cahyadi, and Yeon Ho Chung. High-speed optical camera v2v communications using selective capture. *Photonic Network Communications*, 36(2):210–216, 2018.

[21] Mohammad Shaifur Rahman, Md Mejbaul Haque, and Ki-Doo Kim. Indoor positioning by led visible light communication and image sensors. *International Journal of Electrical and Computer Engineering*, 1(2):161, 2011.

[22] Zhice Yang, Zeyu Wang, Jiansong Zhang, Chenyu Huang, and Qian Zhang. Wearables can afford: Light-weight indoor positioning with visible light. In *Proceedings of the 13th Annual International Conference on Mobile Systems, Applications, and Services*, pages 317–330, 2015.

[23] Md Shahjalal, Moh Hasan, Mostafa Zaman Chowdhury, Yeong Min Jang, et al. Smartphone camera-based optical wireless communication system: requirements and implementation challenges. *Electronics*, 8(8):913, 2019.

[24] Sayaka Nishimoto, Takaya Yamazato, Hiraku Okada, Toshiaki Fujii, Tomohiro Yendo, and Shintaro Arai. High-speed transmission of overlay coding for road-to-vehicle visible light communication using led array and high-speed camera. In *2012 IEEE Globecom Workshops*, pages 1234–1238. IEEE, 2012.

[25] Michael W. Davidson. Concepts and formulas in microscopy resolution. [EB/OL]. https://www.microscopyu.com/microscopy-basics/resolution Accessed July 31, 2021.

[26] Lord Rayleigh. Xxxi. investigations in optics, with special reference to the spectroscope. *The London, Edinburgh, and Dublin Philosophical Magazine and Journal of Science*, 8(49):261–274, 1879.

[27] Kevin Liang, Chi-Wai Chow, and Yang Liu. Rgb visible light communication using mobile-phone camera and multi-input multi-output. *Optics express*, 24(9):9383–9388, 2016.

[28] Nobuyuki Otsu. A threshold selection method from gray-level histograms. *IEEE transactions on systems, man, and cybernetics*, 9(1):62–66, 1979.

[29] Satoshi Suzuki et al. Topological structural analysis of digitized binary images by border following. *Computer vision, graphics, and image processing*, 30(1):32–46, 1985.

[30] M. Born, P. C. Clemmow, D. Gabor, A. R. Stokes, A. M. Taylor, P. A. Wayman, and W. L. Wilcock. Principles of optics. *Pergamon Press*, 1959.

[31] Introduction to light emitting diodes (leds). [EB/OL]. https://engineering.purdue.edu/~ece495/Power_Electronics_Lab/LED_Basics.pdf Accessed July 31, 2021.

[32] WorldSemi. Ws2812b intelligent control led integrated light source. [EB/OL]. https://cdn-shop.adafruit.com/datasheets/WS2812B.pdf Accessed July 31, 2021.

[33] Canon. Eos 5d mark iv. [EB/OL]. https://gdlp01.c-wss.com/gds/0/0300024970/01/eos5d-mk4-im-en.pdf Accessed July 31, 2021.

[34] DJI. Zenmuse-h20. [EB/OL]. https://www.dji.com/zenmuse-h20-series Accessed July 31, 2021.

[35] GSMARENA. iphone x specification. [EB/OL]. https://www.gsmarena.com/apple_iphone_x-8858.php Accessed July 31, 2021.

[36] Mostafa Zaman Chowdhury, Md Tanvir Hossan, Amirul Islam, and Yeong Min Jang. A comparative survey of optical wireless technologies: Architectures and applications. *ieee Access*, 6:9819–9840, 2018.

[37] Yining Wang, Mingzhe Chen, Zhaohui Yang, Tao Luo, and Walid Saad. Deep learning for optimal deployment of uavs with visible light communications. *IEEE Transactions on Wireless Communications*, 19(11):7049–7063, 2020.

[38] Sridhar Rajagopal, Richard D Roberts, and Sang-Kyu Lim. Ieee 802.15.7 visible light communication: modulation schemes and dimming support. *IEEE Communications Magazine*, 50(3):72–82, 2012.